

**SUPPLEMENTARY MATERIALS
FOR
COASTAL CLIMATE VARIABILITY IN NORTHEAST GREENLAND AND THE ROLE OF CHANGING
SEA AND FJORD ICE**

Sonika Shahi^{1,2}, Jakob Abermann^{1,2,3}, Tiago Silva^{1,2}, Kirsty Langley³, Signe Hillerup Larsen⁴, Mikhail Mastepanov⁵, Wolfgang Schöner^{1,2}

¹Department of Geography and Regional Science, University of Graz, Graz, Austria

²Austrian Polar Research Institute, Vienna, Austria

³Asiaq-Greenland Survey, Nuuk, Greenland

⁴Geological Survey of Denmark and Greenland, Copenhagen, Denmark

⁵Aarhus University, Aarhus, Denmark

Correspondence to: Sonika Shahi (sonika.shahi@uni-graz.at)

Content of this file: Figures S1–S17 and Tables S1–S6

SUPPLEMENTARY FIGURES

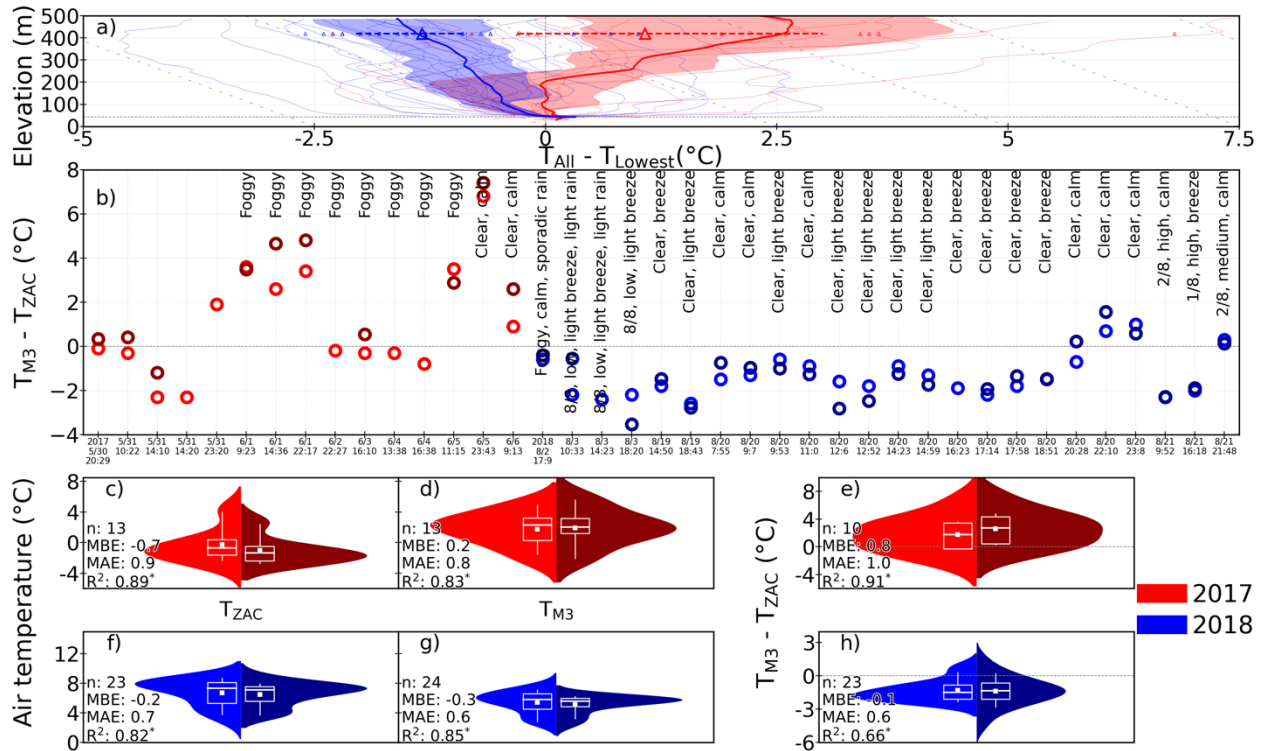


Figure S1. Comparison of free-air and near-surface temperatures at the same level. (a) Vertical temperature profiles normalized with respect to temperature at the lowest elevation (T_{Lowest}) as measured with the UAV. The mean normalized temperature profiles (bold lines) are calculated from 40 (16 from 2017, red; 24 from 2018, blue) sub-daily normalized vertical temperature measurements (thin line) from UAV. The mean normalized temperature (big triangle) at M3 is calculated from sub-daily temperatures (small triangle) normalized with respect to temperature at ZAC for the temporally overlapping UAV measurement periods. The shaded region (around the bold line) and dashed line (through the triangle) indicate the 25th and 75th percentiles of UAV and AWS measurements, respectively. The mean environmental lapse rate (grey dashed line) of $6.5^{\circ}C km^{-1}$ is plotted for reference. (b) Difference between sub-daily temperatures at M3 (T_{M3} ; 420 m) and ZAC (T_{ZAC} ; 43 m) elevations representing surface (from AWS; light color) and free-air (from UAV; dark color) temperature differences. Markers above the zero line represent temperature inversions. Weather conditions at the time of the UAV flights recorded by the observers are shown where available. (c–h) Frequency distribution (n is the sample size) of T_{M3} and T_{ZAC} (c, d, f, and g) and differences among them (e and h) measured by AWS (light color) and UAV at the same elevation (dark color) for 2017 (red) and 2018 (blue). The difference between temperature measured by UAV and AWS at the same elevation is indicated by metrics like mean bias error (MBE), mean absolute error (MAE) and, coefficient of determination (R^2) (* represents $p < 0.05$). Box-and-whisker plots show the median (white horizontal line), the mean (white square), the 25th and 75th percentiles (bottom and top of the box), and the 5th and 95th percentiles (whiskers; white line) for the temperature at ZAC and M3 and differences among them.

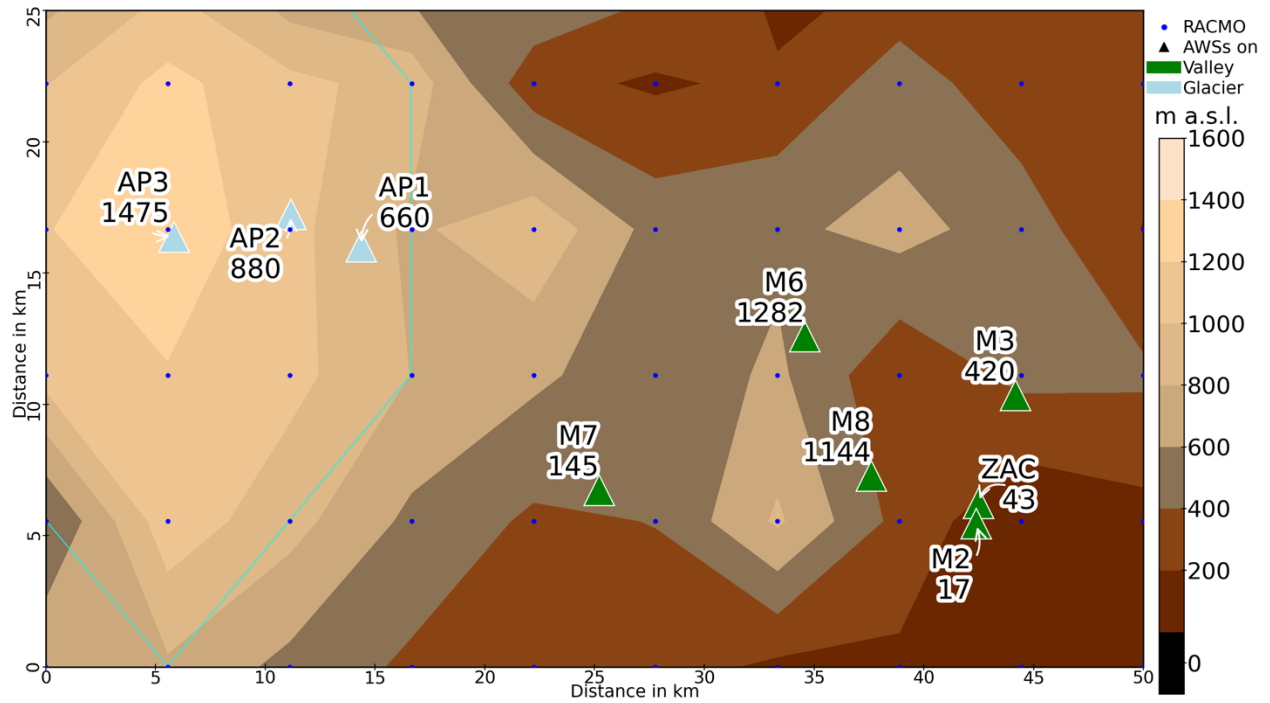


Figure S2. RACMO topographic map showing the Zackenberg region. Triangles represent the automatic weather stations (AWSs) on the ice-free surface (green) and A. P. Olsen Ice Cap (blue). Cyan contour represents the peripheral glacier mask from the Programme for Monitoring the Greenland Ice Sheet (PROMICE), upscaled and used in RACMO. Color bar represents elevation in meters above mean sea level (m a.s.l.). The blue dot represents RACMO grid point of 5.5 km horizontal resolution.

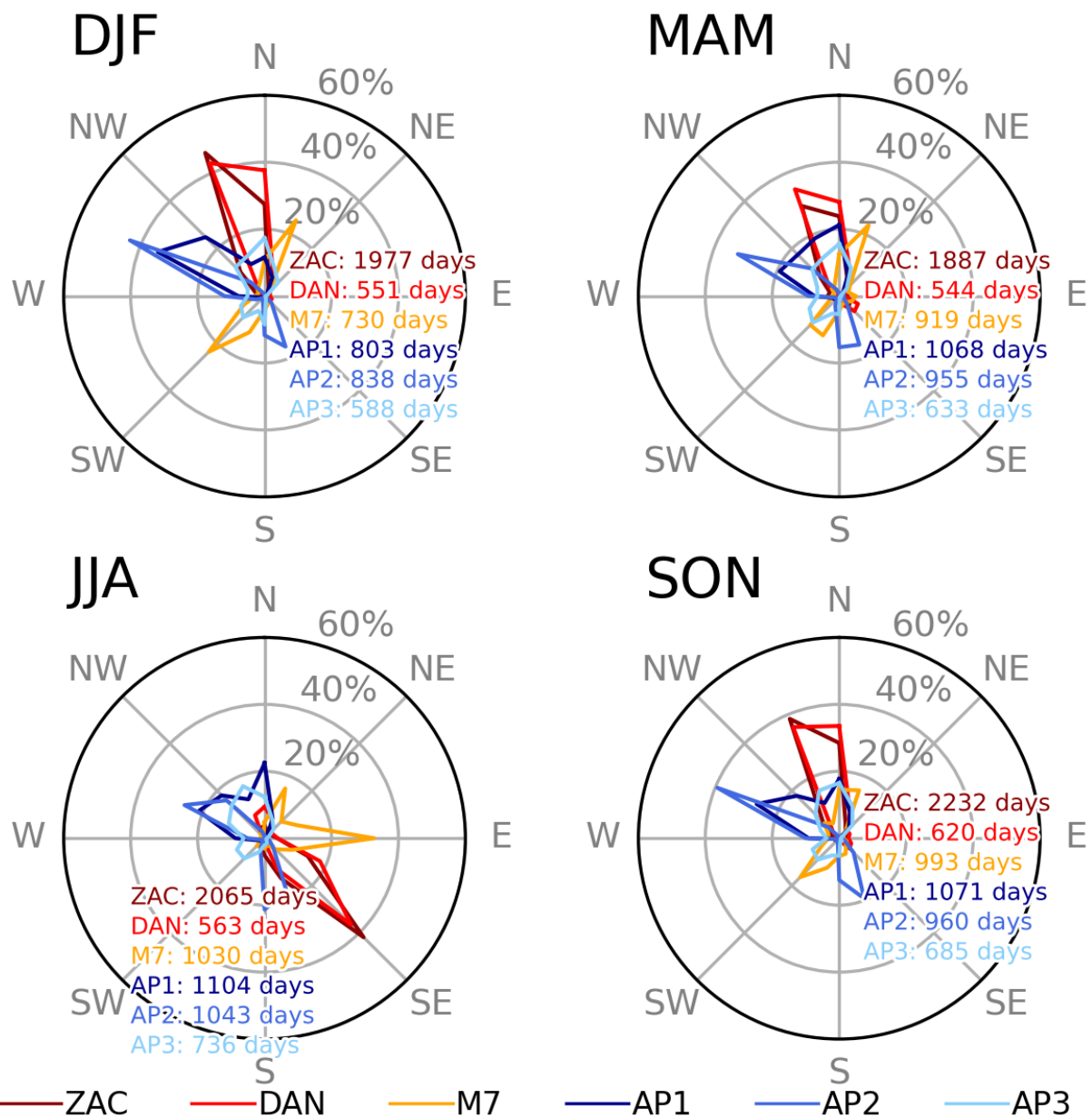


Figure S3. Wind rose showing a seasonal frequency of wind direction measured by given AWS. The frequency of wind blowing from a certain direction is expressed as percentage over the entire season calculated from all available daily records (indicated in legend). For stations on A. P. Olsen Ice Cap, the down-glacier direction is around 293–315°.

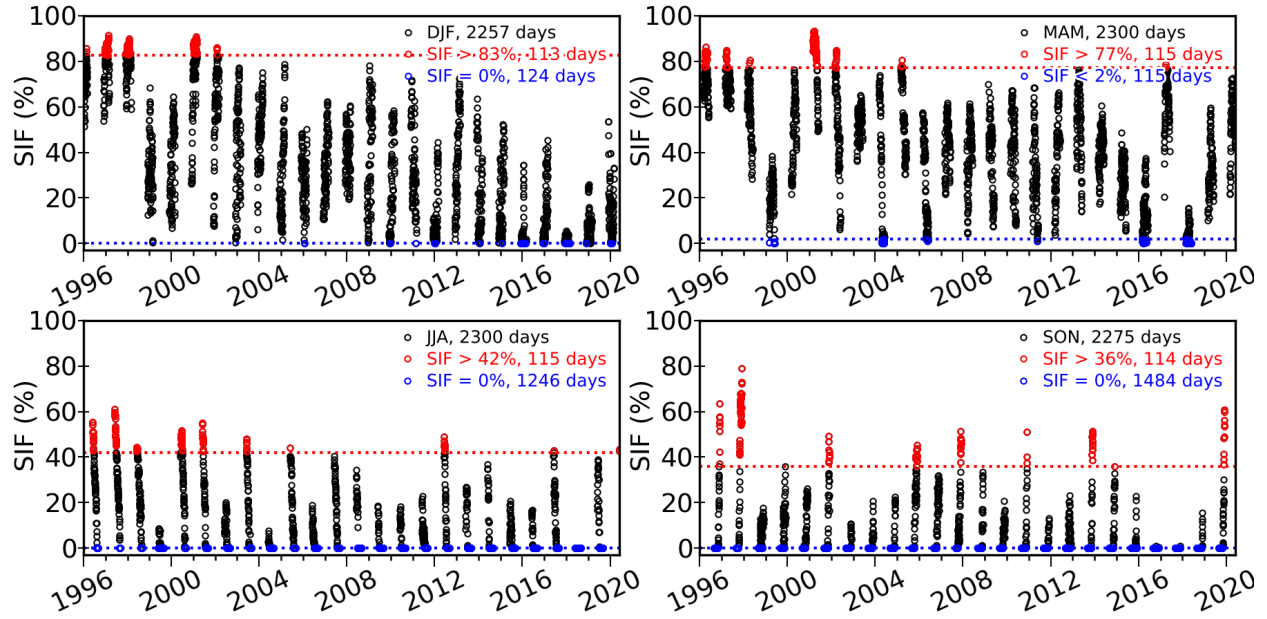


Figure S4. The time series of daily fractional sea-ice cover (SIF in %) zonally (overall grid cells) averaged (median) over the Greenland Sea for entire daily measurements for the given season (1996–2020). A circle marker represents the SIF for all days (black circle), high days (red circle; days when SIF is more than 95th percentile), and low days (blue circle; the days when SIF is less than or equal to (when SIF_{5th} is equal to zero) 5th percentile of SIF) over the period 1996–2020. The red and blue dashed lines represent the 95th and 5th percentiles of SIF, respectively, for the given season.

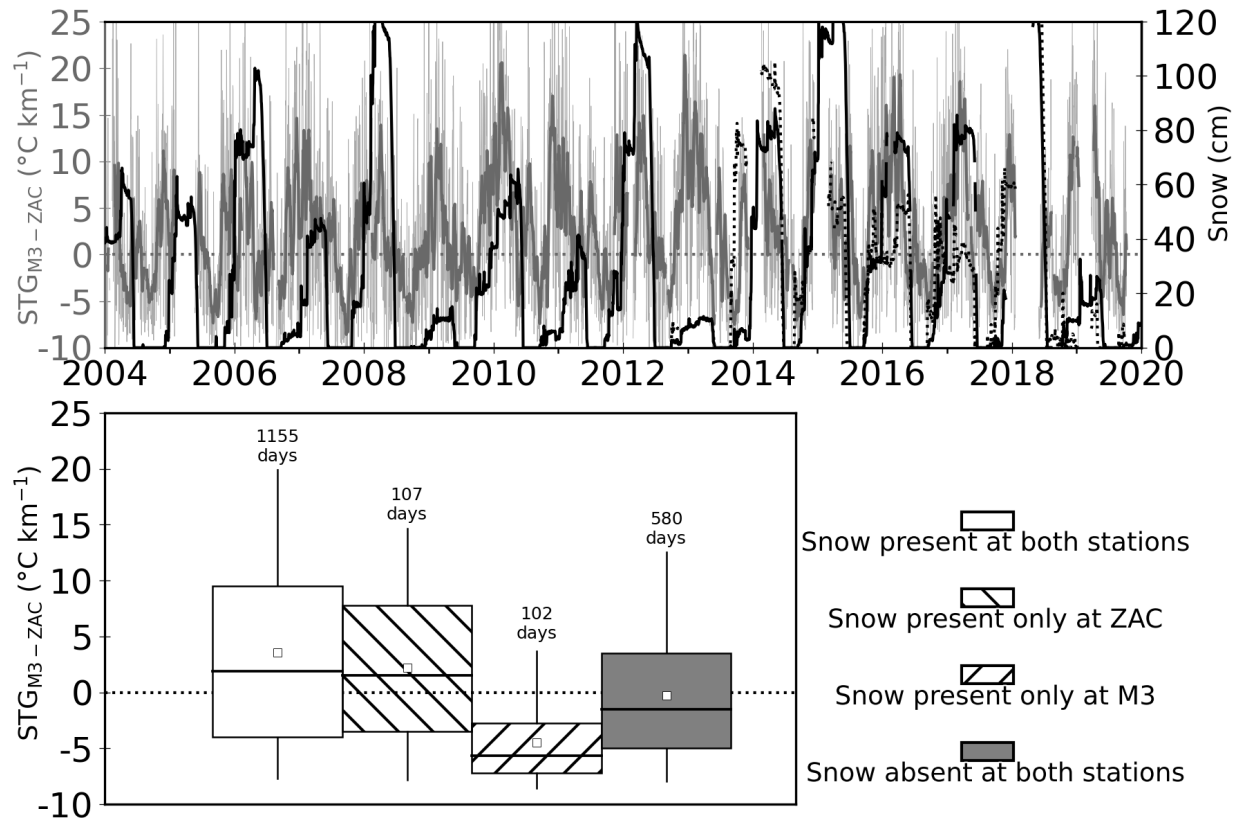


Figure S5. Relationship between daily STG and snow depth. The upper panel represents the time series of daily mean STG between M3 and ZAC (STG_{M3-ZAC} in $^{\circ}C km^{-1}$), (light gray line), and snow depth (cm) recorded at ZAC (solid black line) and M3 (dashed black line) for available measurement period (2004–2020). The dark grey line represents 15 days rolling mean of STG_{M3-ZAC} . The lower panel indicates box plots of daily mean STG_{M3-ZAC} when snow is present at both stations (white box), snow is present only at ZAC (backward hatch), snow is present only at M3 (forward hatch), and snow is absent at both stations (gray box) during the measurement period. Box-and-whisker plots show the mean (white square), the median (black horizontal line), the 25th and 75th percentiles (bottom and top of the box), and the 5th and 95th percentiles (whiskers; black line) for daily STG_{M3-ZAC} . The total number of days satisfying the given conditions is displayed at top of the uppermost whisker (which represents the 95th percentile).

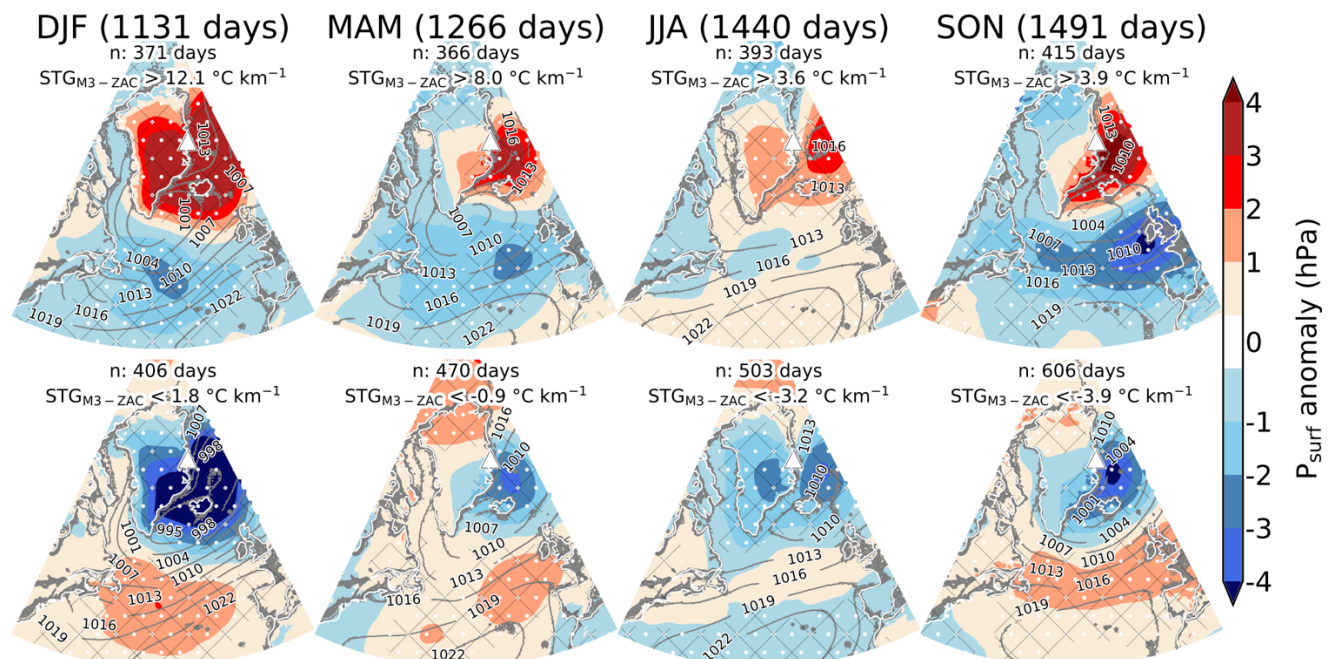


Figure S6. Composite of surface pressure (P_{surf} in hPa) anomalies (shading) and means (gray contours; 3 m interval) from ERA5 corresponding to the STG between M3 and ZAC ($\text{STG}_{\text{M3-ZAC}}$) for entire daily measurements (number of days indicated at the top of each seasonal column) for a given season (2004–2019). The upper and lower panels represent P_{surf} anomalies corresponding to high and low STG days i.e., n number of days when $\text{STG}_{\text{M3-ZAC}}$ exceed and is less than the indicated STG values in $^{\circ}\text{C km}^{-1}$, respectively, for the given season. The triangle represents the location of the Zackenberg region. The white dots and areas within the black mesh indicate statistically significant differences between high and low composite anomalies at the 0.05 and 0.1 significance levels, respectively.

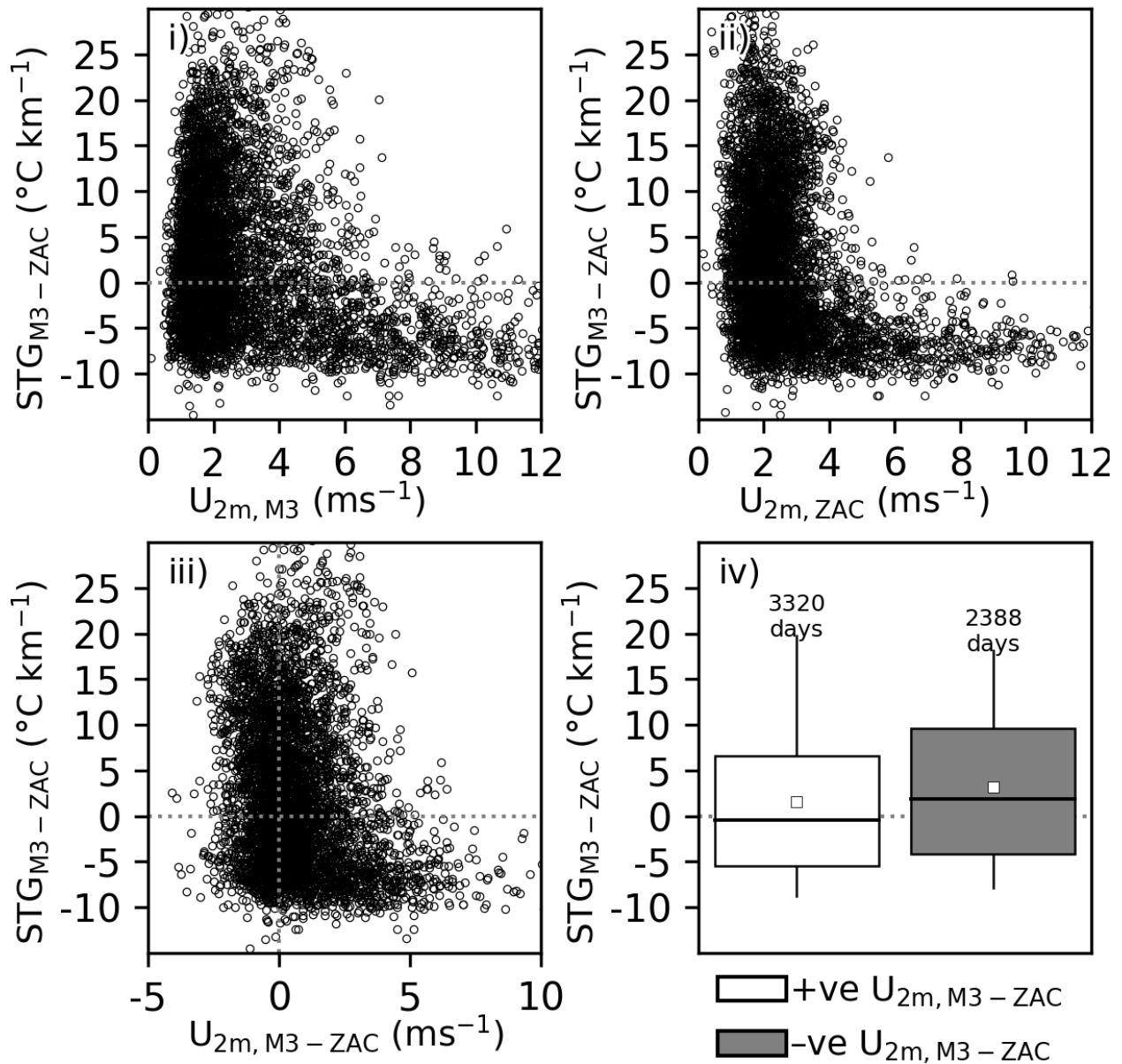


Figure S7. Relationship between daily STG and wind speed (U_{2m}) observed at M3 and ZAC: i) and ii) daily STG between M3 and ZAC (STG_{M3-ZAC} in °C km⁻¹) versus U_{2m} at M3 and ZAC, respectively; iii) daily STG_{M3-ZAC} versus wind shear; iv) Box plots of daily mean STG_{M3-ZAC} when wind shear is positive (white box) and negative (grey). The total number of days satisfying the given conditions is displayed at top of the uppermost whisker (which represents the 95th percentile).

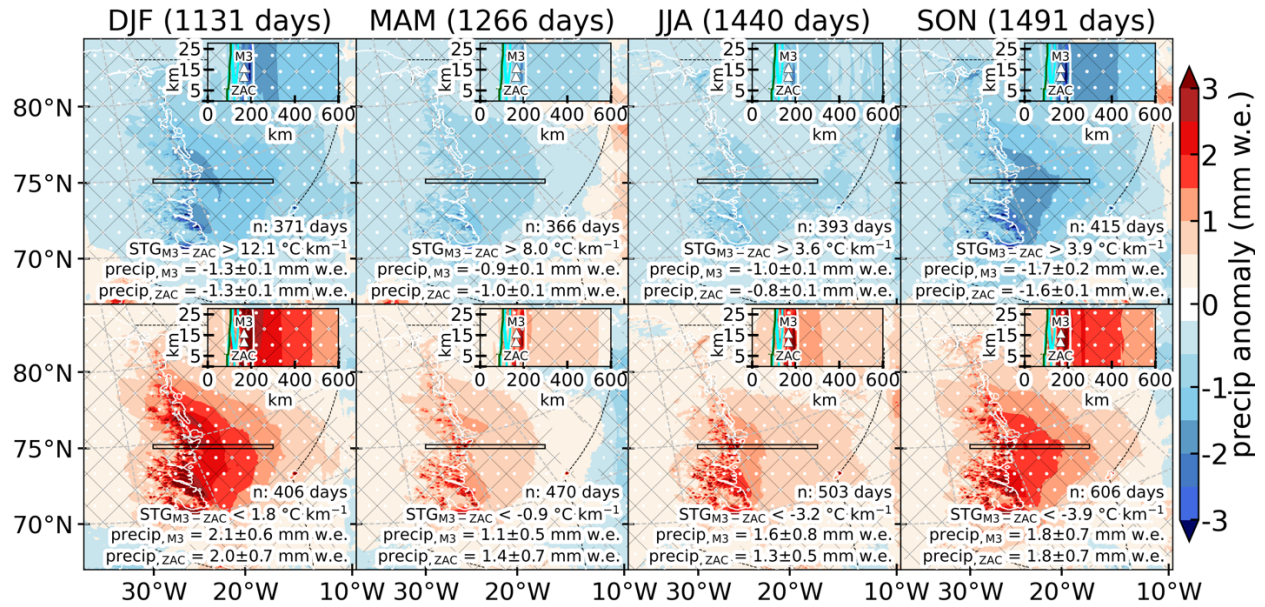


Figure S8. Idem as Figure S6 but for the composites of precipitation (precip in mm w.e.) anomalies from RACMO. The inset figure shows the zoomed-in version of the black rectangle in the main figure and Fig. 1 encompassing the ZR; the location of the stations (triangle), the land-sea border (white contour), peripheral glacier (cyan contour), and the GrIS (green contour) are indicated in the inset figure. The dashed black line represents the GrSea coverage. The mean precipitation anomaly values (in mm w.e.) interpolated to the station location are also shown in the lower right corner indicating a 95 % confidence interval (calculated using bootstrapping methods). The white dots and areas within the black mesh indicate statistically significant differences between high and low composite anomalies at the 0.05 and 0.1 significance levels, respectively.

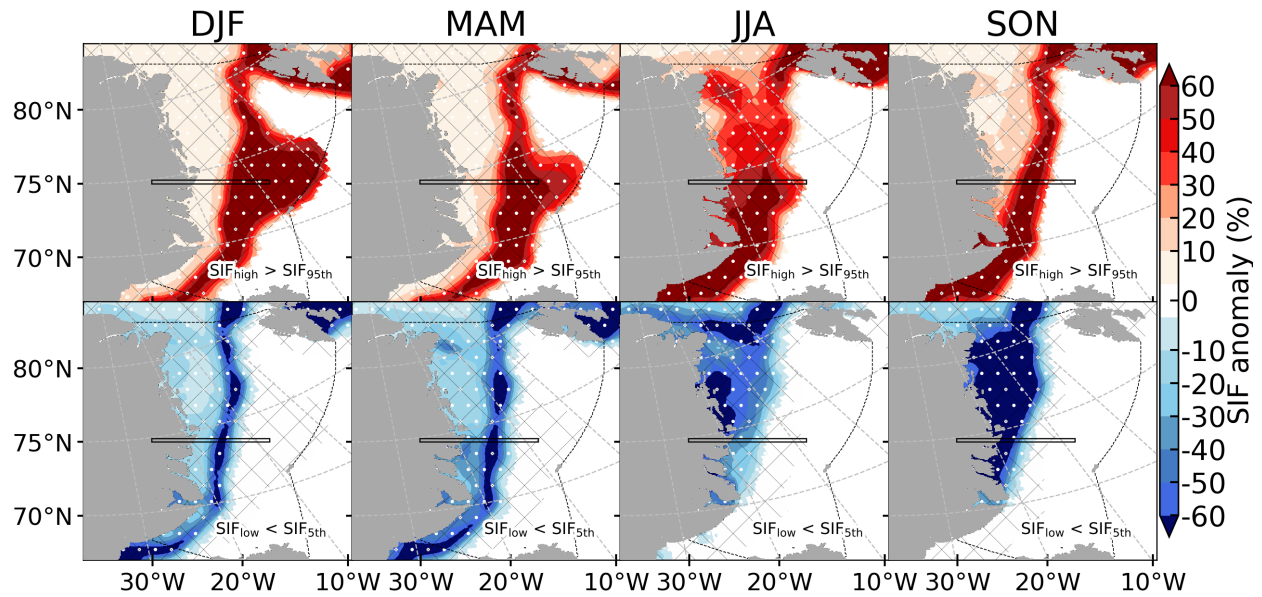


Figure S9. Composites of fractional sea-ice cover anomaly (SIF in %) from ERA5 for 1996–2020. Each grid point represents high (upper panel) and low (lower panel) SIF anomalies when SIF is more than 95th and less than the 5th percentile of SIF for the given period, respectively. The white dots and areas within the black mesh indicate statistically significant differences between high and low composite anomalies at the 0.05 and 0.1 significance levels, respectively.

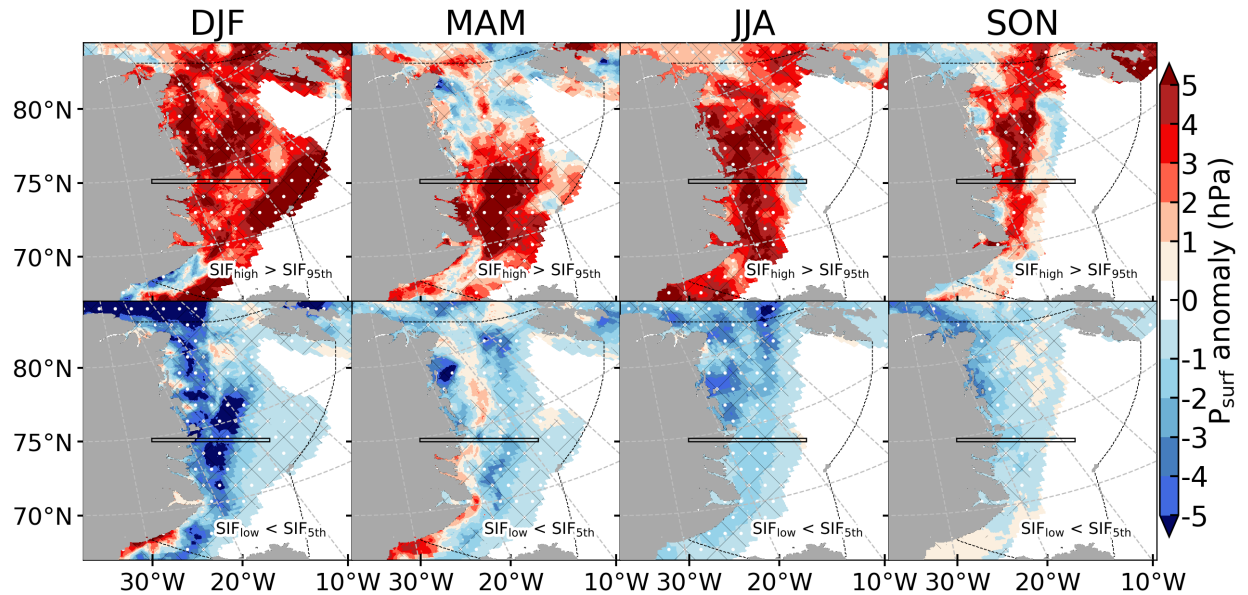


Figure S10. Composites of surface pressure anomaly (P_{surf} in hPa) from RACMO corresponding to the SIF anomalies shown in Figure S9 for the given season (1996–2020). Each grid point represents cases when SIF exceeds the 95th percentile (upper panel) and is less than the 5th percentile (lower panel) of SIF for the given period. The white dots and areas within the black mesh indicate statistically significant differences between high and low composite anomalies at the 0.05 and 0.1 significance levels, respectively.

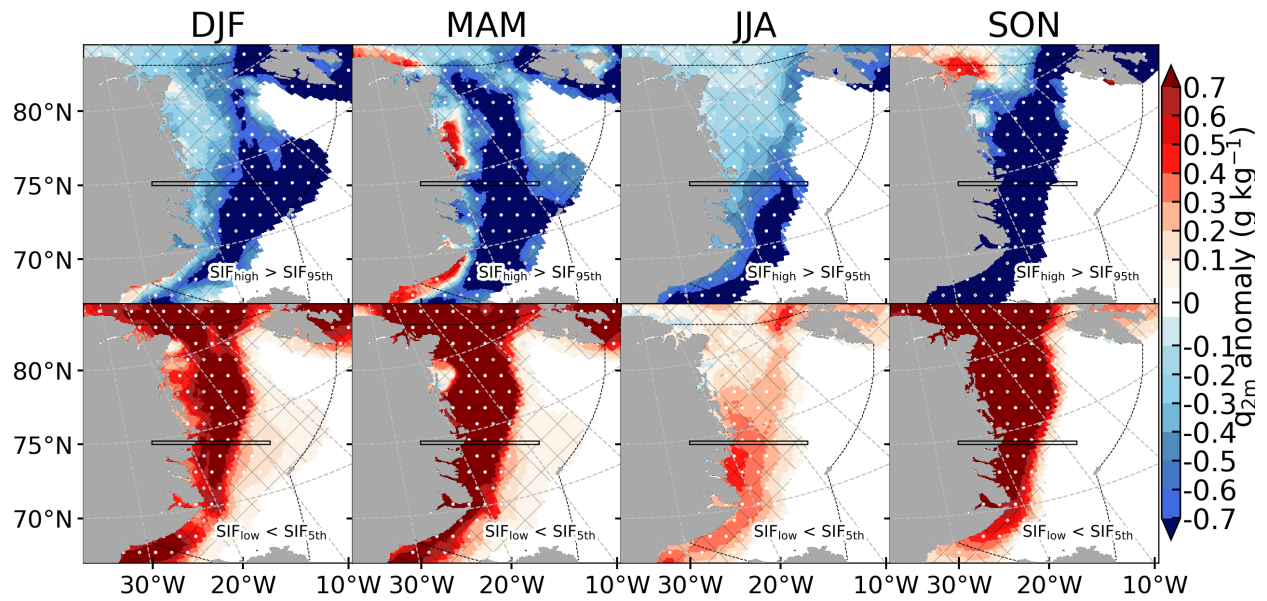


Figure S11. Idem as Figure S10, but for the composites of specific humidity (q_{2m} in $g\ kg^{-1}$) anomaly from RACMO.

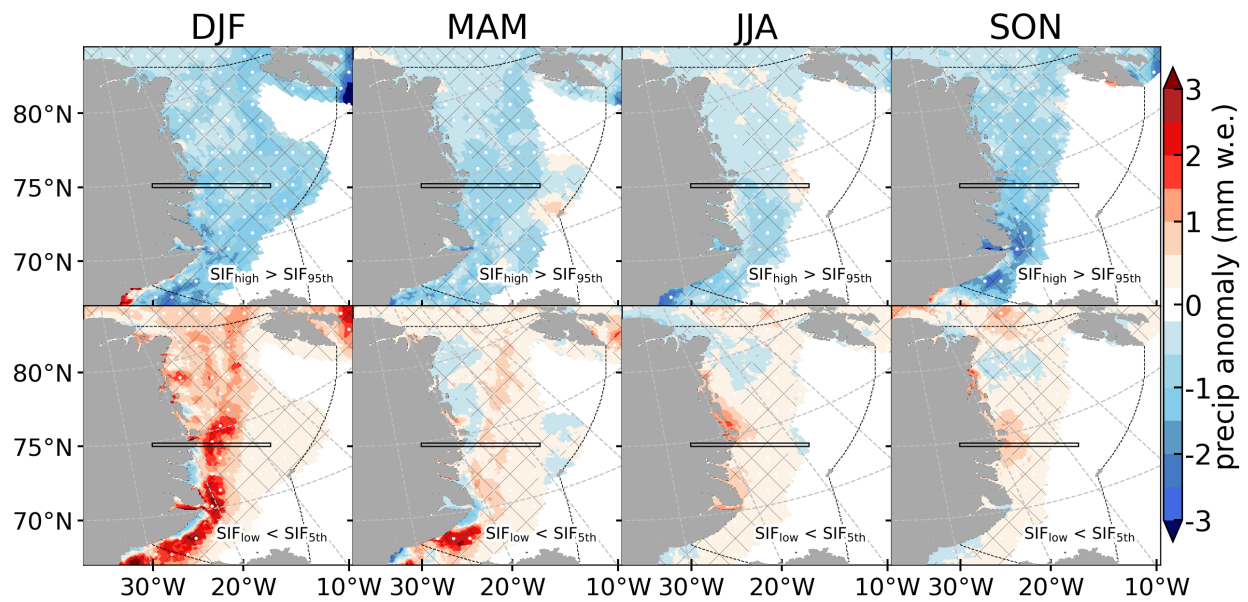


Figure S12. Idem as Figure S10, but for the composites of precipitation (precip in mm w.e.) anomaly from RACMO.

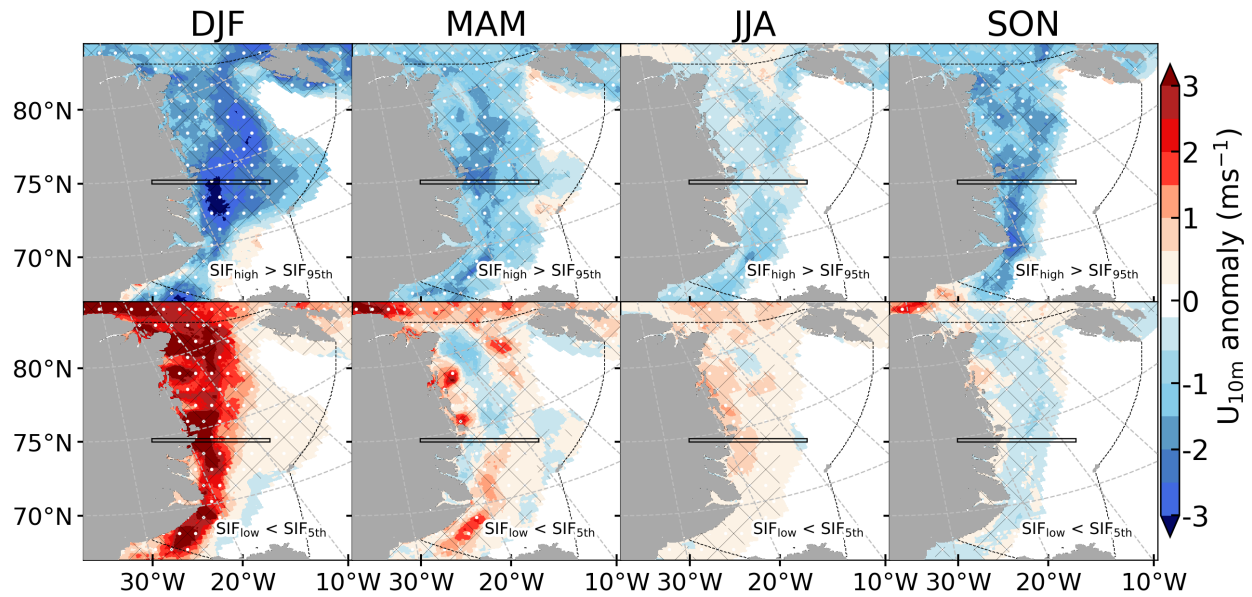


Figure S13. Idem as Figure S10, but for the composites of wind speed (U_{10m} in $m s^{-1}$) anomaly from RACMO.

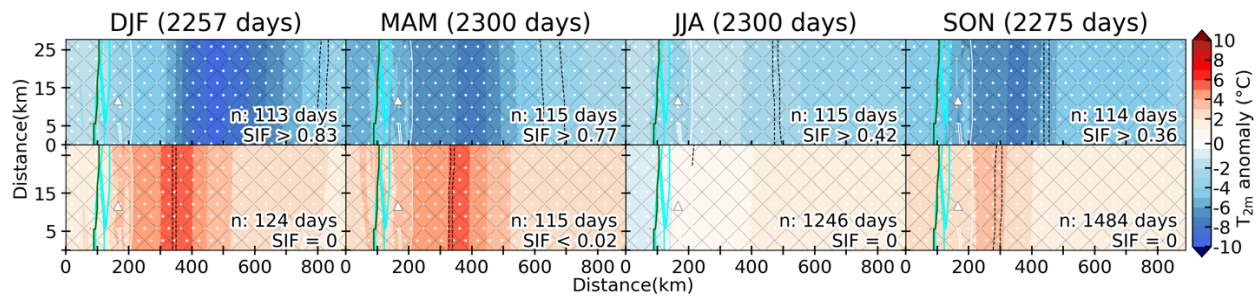


Figure S14. Composite of 2-m air temperature (T_{2m} in $^{\circ}C$) anomalies from RACMO corresponding to zonally (overall grid cells) averaged (median) SIF over the Greenland Sea for entire daily measurements for the given season (1996–2020). The upper and lower panels represent T_{2m} anomalies corresponding to high and low SIF days i.e., n number of days when SIF exceed and is less than or equal to the indicated SIF values, respectively, for each season. The figure is the zoomed-in version of the black rectangle in Fig. 1 encompassing the ZR; the location of the stations (triangle), the land-sea border (white contour), peripheral glacier (cyan contour), and the GrIS (green contour) are indicated. The average sea-ice extent (dashed black line) for the given condition is also shown; the outer line represents 0.25 SIF and the inner line 0.3. The white dots and areas within the black mesh indicate statistically significant differences between high and low composite anomalies at the 0.05 and 0.1 significance levels, respectively.

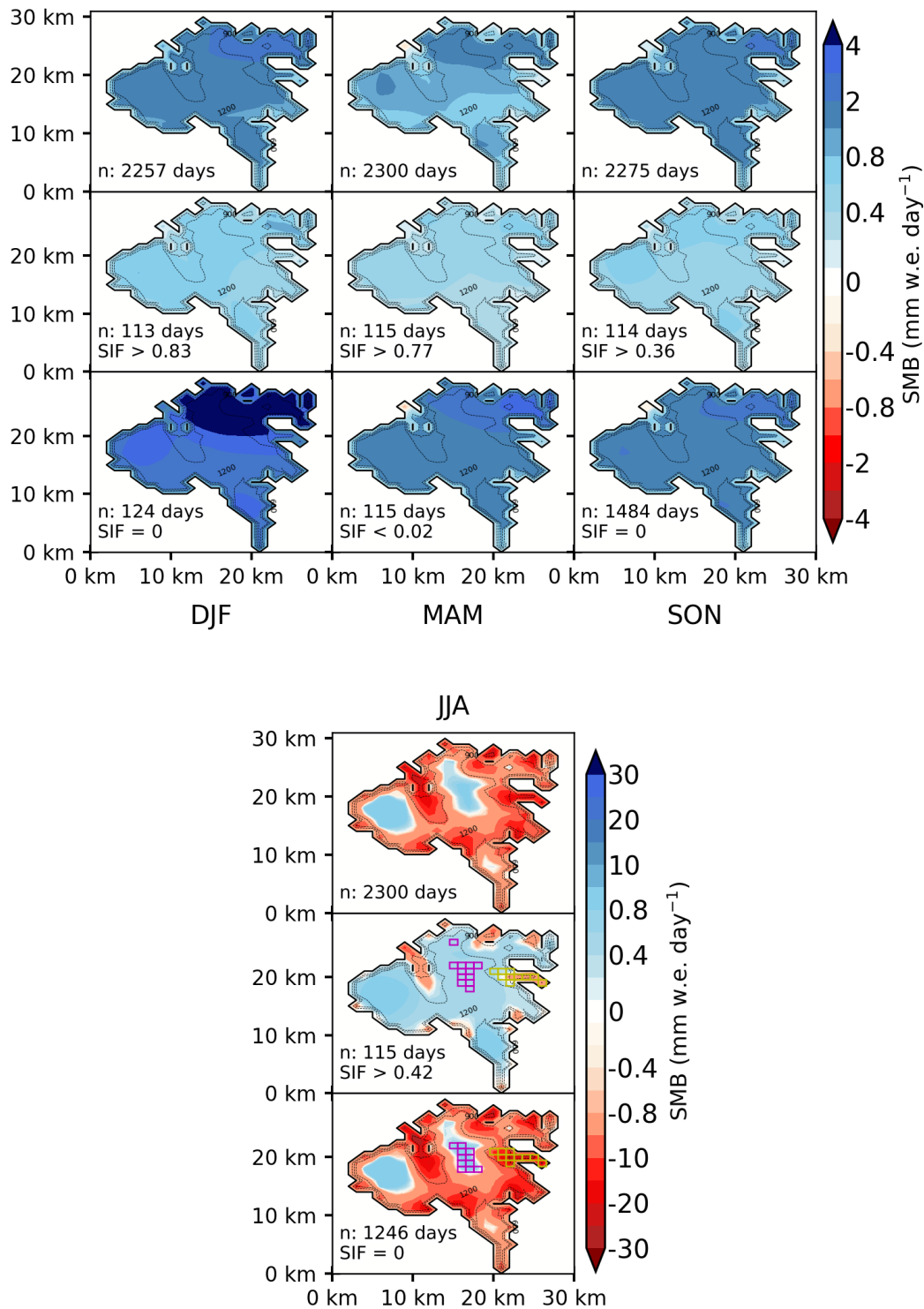


Figure S15. Mean composites of daily surface mass balance (SMB in mm w.e. day⁻¹) of A. P. Olsen Ice Cap (APO), (location in Fig. 1) from RACMO corresponding to SIF averaged over the Greenland Sea for entire daily measurements for the given season (1996–2020). For each season, upper, middle, and lower panels represent the daily mean SMB corresponding to all days, high, and low SIF days i.e., all n number of days, n number of days when SIF exceeds and is less than or equal to the indicated SIF values, respectively. In JJA panel, the magenta and yellow rectangles indicate the grid cells whose values are used for the calculation of the daily mean SMB on accumulation (>1100 m a.s.l.) and ablation (<1100 m a.s.l.; only the southeastward flowing outlet glacier) area, respectively, of the APO. Note the use of a separate color bar for summer composite due to large mass overturn.

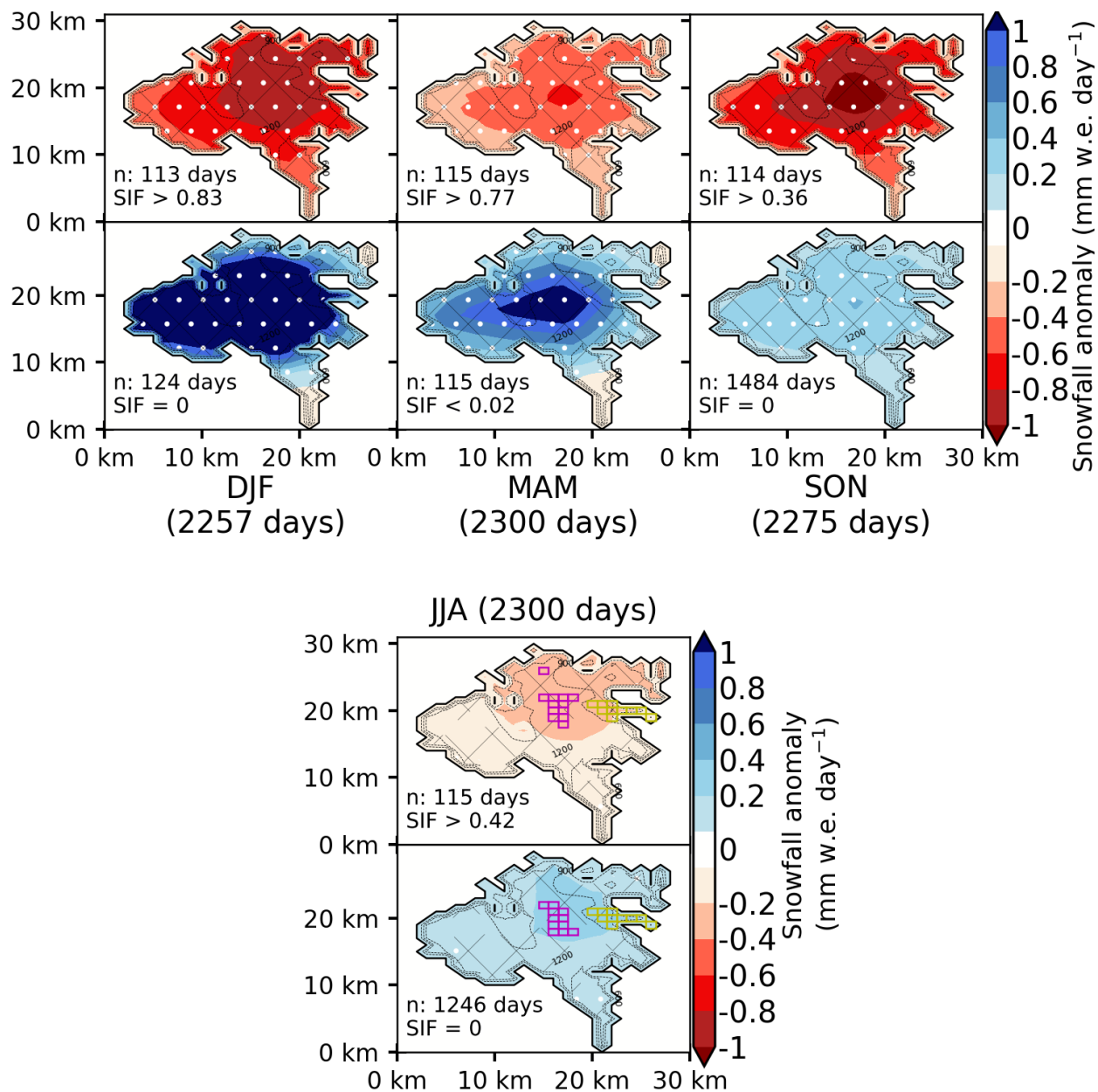


Figure S16. Composites of daily snowfall anomaly (in mm w.e. day⁻¹) over A. P. Olsen Ice Cap (APO) from RACMO corresponding to SIF averaged over the Greenland Sea for entire daily measurements for the given season. For each season, upper and lower panels represent snowfall anomalies corresponding to high and low SIF days i.e., n number of days when SIF exceeds and is less than or equal to the indicated SIF values, respectively. In JJA panel, the magenta and yellow rectangles indicate the grid cells whose values are used for the calculation of the average snowfall anomaly on accumulation (>1100 m a.s.l.) and ablation (<1100m a.s.l.; only the southeastward flowing outlet glacier) area, respectively, of the APO. The white dots and areas within the black mesh indicate statistically significant differences between high and low composite anomalies at the 0.05 and 0.1 significance levels, respectively.

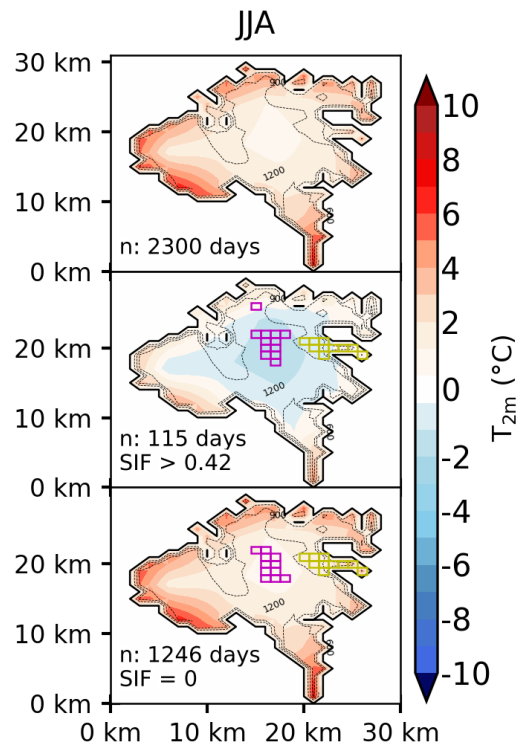
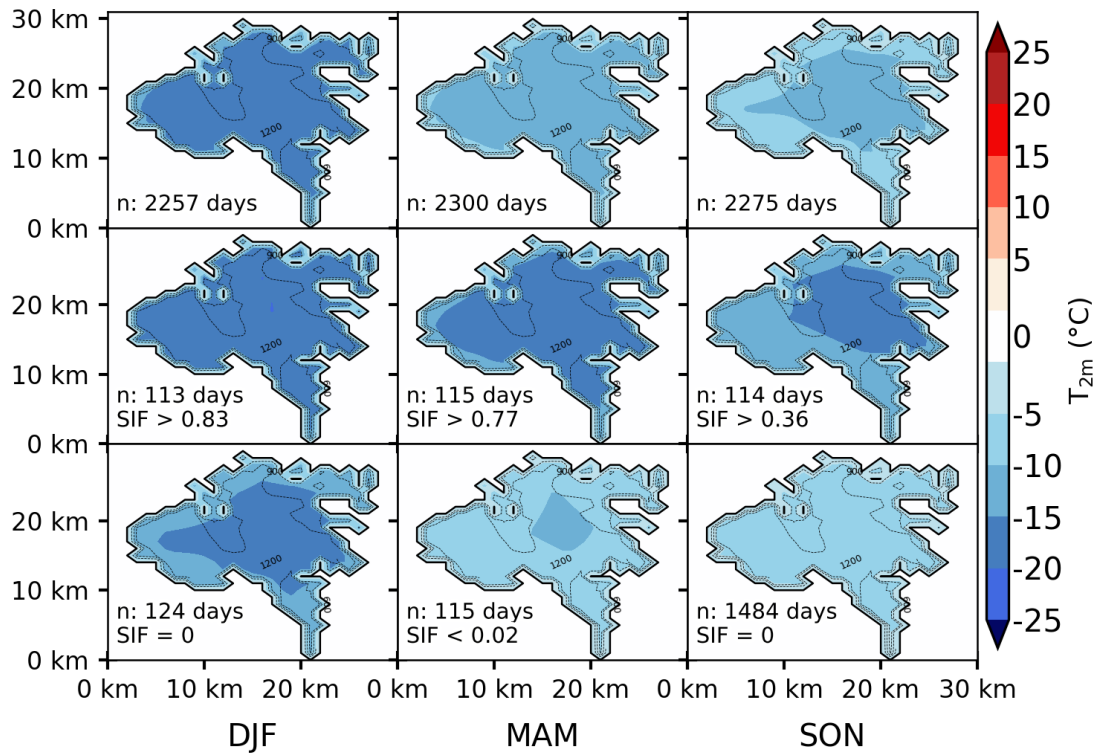


Figure S17. Idem as Figure S15, but for the mean composites of daily 2-m air temperature (T_{2m} in $^{\circ}\text{C}$) of A.P. Olsen Ice Cap (location in Fig. 1) from RACMO.

SUPPLEMENTARY TABLES

Table S1. Instrumentation used at the AWSs (Skov et al., 2019; Kandrup and Iversen, 2010; Citterio et al., 2015). Numbers in parentheses indicate the sensor height in meters above the surface. Note that the temperature at ZAC is measured at two heights: 2 m and 7.5 m. Instrument specifications are not available for M6 and DAN stations.

Variables	ZAC	M2, near ZAC	M3, Aucellabjerg	M7, Store SØdal	M8, Zackenberg mountain	AP1, AP2 and AP3
Air temperature (°C) and relative humidity (%)	Vaisala, HMP 45D (2 and 7.5 m) (± 0.3 °C / $\pm 2\%$ for 0–90% RH $\pm 3\%$ for 90–100% RH)	Campbell, MP103A and Rotronic, HC2S3 (2.5 m)	Campbell, MP103A and Rotronic, HC2S3 (2 m)	Rotronic HC2S3	Vaisala, VXT536	Rotronic MP102H with Pt100 and HC2-S3 probe (2.7), (± 0.1 °C / $\pm 0.8\%$)
Wind speed (ms^{-1}) and direction (°)	Met One 034B (2 and 7.5 m) ($\pm 5^\circ$)	Young, 05103-45 (2.5 m)	Young, 05103-45 (2 m)	Young, 05103-45 (2 m)	Vaisala, VXT536	R.M. Young 05103-5 (3), (± 0.3 ms^{-1} , $\pm 3^\circ$)
Atmospheric pressure at the surface (hPa)	Vaisala, PTB101B (1.6 m) (± 0.15 hPa)	–	–	–	Vaisala, VXT536	Setra model 278 (± 2.5 hPa)
Radiometer (Wm^{-2})	Kipp & Zonen, CM7B and NR. Lite (2 m) ($\pm 1\%$)	Kipp & Zonen, CNR4 (2.5 m)	Kipp & Zonen, CNR1(2 m)	–	–	Kipp & Zonen, CNR4 (3), ($<5\%$ SWR, $<10\%$ LWR)
Snow depth (mm)	Campbell Scientific, SR50-45 (2 m) (± 1 cm or 0.4% of distance to target)	Campbell Scientific, SR50a (2.5 m)	Campbell Scientific, SR50a (1.8 m)	Campbell Scientific, SR50a	–	Campbell Scientific SR50 or SR50A (± 1 cm)

Table S2. The manufacturer's specifications for iMET-XQ2 sensors. Datasheet for sensor package is available at iMet XQ2 (iMet-XQ2 Second-Generation Atmospheric Sensor for UAV Deployment, 2021).

	Type	Range	Response time	Accuracy	Resolution
Temperature sensor	Bead Thermistor	-90 – +50 °C	1 second at 5 m s^{-1} flow	± 0.3 °C	0.01 °C
GPS	UBlox CAM-M8	-	1 second	12 m (Vertical)	-

Table S3. Evaluation statistics of daily modeled meteorological variables like 2-m air temperature (T_{2m}), specific humidity (q_{2m}), 10-m wind speed (U_{10m}), and surface pressure (P_{surf}) using daily mean measurements collected at all AWSs in the Zackenberg region for all seasons. The error metrics like the coefficient of determination (R^2), mean bias error (MBE), mean absolute error (MAE), and root-mean-square-errors (RMSE) are provided for all AWSs. The observed and modeled elevation difference is also shown. Note that the measured wind speed (U_{2m}) is at 2 m, while RACMO's wind speed is modeled at 10 m.

T_{2m} (°C)																
	DJF				MAM				JJA				SON			
	R^2	MBE	MAE	RMSE	R^2	MBE	MAE	RMSE	R^2	MBE	MAE	RMSE	R^2	MBE	MAE	RMSE
ZAC	0.7	4.4	5	6.1	0.8	3.7	4	5	0.7	0.6	1.5	2	0.8	1.8	2.7	3.8
M2	0.6	4.6	5.2	6.4	0.8	3.6	3.8	4.9	0.7	1	1.7	2.3	0.8	1.5	2.6	3.6
M3	0.8	0.2	2	2.6	0.9	0.4	1.6	2.1	0.8	-1	1.6	2.1	0.9	-0.3	1.6	2
M7	0.5	4.3	5.1	6.4	0.8	3.8	4.1	5	0.7	1.8	2.3	3	0.8	2	3.1	4.1
M6	0.7	1.1	2.7	3.3	0.9	1.5	2.6	3.1	0.7	1.7	2.3	2.7	0.8	2.2	3	3.4
AP1	0.8	1.1	2.6	3.1	0.9	2.5	3	3.4	0.5	2.2	3	3.4	0.8	3.6	3.8	4.3
AP2	0.8	-0.8	2.5	3	0.9	1.9	2.4	2.9	0.8	1.6	2	2.5	0.9	1	2.1	2.6
AP3	0.8	1.5	2.2	2.7	0.9	-0.3	1.8	2.3	0.8	-1.3	1.5	1.8	0.8	-1	2.2	2.8
q_{2m} (g kg ⁻¹)																
	DJF				MAM				JJA				SON			
	R^2	MBE	MAE	RMSE	R^2	MBE	MAE	RMSE	R^2	MBE	MAE	RMSE	R^2	MBE	MAE	RMSE
ZAC	0.7	0.1	0.3	0.4	0.8	0.3	0.4	0.5	0.6	0	0.4	0.5	0.8	0.1	0.3	0.4
M6	0.7	-0.1	0.2	0.3	0.8	0.2	0.3	0.5	0.5	0.6	0.7	0.9	0.8	0.1	0.3	0.4
AP1	0.8	-0.1	0.2	0.2	0.9	0.3	0.3	0.5	0.6	0.4	0.5	0.7	0.9	0.1	0.3	0.4
AP2	0.8	-0.1	0.2	0.2	0.8	0.2	0.3	0.4	0.7	0.2	0.4	0.5	0.9	0	0.3	0.3
AP3	0.7	0	0.2	0.2	0.8	0.2	0.3	0.4	0.6	0.5	0.6	0.7	0.8	0.1	0.3	0.4
U_{10m} (m s ⁻¹)																
	DJF				MAM				JJA				SON			
	R^2	MBE	MAE	RMSE	R^2	MBE	MAE	RMSE	R^2	MBE	MAE	RMSE	R^2	MBE	MAE	RMSE
ZAC	0.5	0.5	1.3	1.7	0.4	0.6	1.1	1.5	0.4	0	0.6	0.9	0.5	0.2	1	1.4
M2	0.5	0.6	1.2	1.7	0.5	0.7	1	1.4	0.4	-0.1	0.6	0.9	0.4	0	1	1.4
M3	0.5	0.4	2.2	2.9	0.3	0.7	1.9	2.5	0.5	-0.1	0.9	1.2	0.3	0.1	1.9	2.5
M7	0.3	-1.8	2.1	3	0.2	-1.7	2	2.7	0.3	-2	2	2.3	0.3	-1.7	2	2.6
M6	0.5	-3.2	3.5	4.5	0.2	-2.6	2.9	3.9	0.2	-1.8	2	2.5	0.4	-3.7	3.9	4.9
AP1	0.4	-1.7	2	2.4	0.3	-1	1.4	1.8	0.2	-1.5	1.7	2.1	0.4	-1.7	2	2.3
AP2	0.5	0.3	1.3	1.7	0.3	0.1	1.2	1.5	0.3	-0.8	1.4	1.7	0.5	-0.1	1.2	1.5
AP3	0.3	-0.8	1.8	2.4	0.6	-1.2	1.5	1.9	0.5	-1.5	1.6	2.1	0.5	-1.3	1.8	2.3
P_{surf} (hPa)																
	DJF				MAM				JJA				SON			
	R^2	MBE	MAE	RMSE	R^2	MBE	MAE	RMSE	R^2	MBE	MAE	RMSE	R^2	MBE	MAE	RMSE
ZAC	0.98	1.1	1.7	2.2	0.98	0.7	1.4	1.7	0.98	1.1	1.3	1.5	0.98	1.2	1.5	1.9
M6	0.95	76.3	76.3	76.3	0.9	75.5	75.5	75.5	0.94	70.6	70.6	70.6	0.91	75	75	75
AP1	0.98	-13	13	13.1	0.98	-13.4	13.4	13.4	0.98	-12.9	12.9	13	0.98	-13.2	13.2	13.3

AP2	0.98	-22	22	22.1	0.99	-22.2	22.2	22.2	0.99	-21.4	21.4	21.4	0.99	-21.9	21.9	21.9
AP3	0.98	15.1	15.1	15.1	0.99	14.6	14.6	14.7	0.98	13.4	13.4	13.4	0.98	14.4	14.4	14.5
Elevation bias (m)																
	Observed elevation				Modeled elevation				Observed minus modeled elevation							
ZAC	43				27				-16							
M2	17				27				10							
M3	420				452				32							
M7	145				405				260							
M6	1282				638				-644							
AP1	660				760				100							
AP2	880				1059				179							
AP3	1475				1355				-120							

Table S4. Anomalies of near-surface variables like wind speed (U_{2m} and U_{10m} in $m\ s^{-1}$), specific humidity (q_{2m} in $g\ kg^{-1}$), cloud cover fraction (CCF in %), and 2-m air temperature (T_{2m} in $^{\circ}C$), measured and derived from AWS and RACMO (interpolated) corresponding to high and low slope temperature gradient between M3 and ZAC (STG_{M3-ZAC} in $^{\circ}C\ km^{-1}$) days for the given season. AWS and RACMO anomalies are calculated using the same period i.e., when the variable is recorded by AWS. The AWS which do not record the given variable is not shown. The plus/minus (\pm) values indicate a 95 % confidence interval (calculated using bootstrapping methods).

Station pairs	Seasons	DJF		MAM		JJA		SON	
		High	Low	High	Low	High	Low	High	Low
M3-ZAC	Composites	1131		1266		1440		1491	
	Total days	1131		1266		1440		1491	
	STG (days)	11.8 (371)	-10.9 (406)	11.5 (366)	-8.9 (470)	8.7 (393)	-6.6 (503)	10.7 (415)	-6.8 (606)
$U_{2m, M3}$ $U_{10m, M3}$	AWS	-1.6 \pm 0.1	2.7 \pm 0.4	-0.9 \pm 0.1	1.3 \pm 0.3	-0.5 \pm 0.1	0.7 \pm 0.2	-1.3 \pm 0.1	1.5 \pm 0.3
	RACMO	-1.6 \pm 0.1	1.9 \pm 0.3	-0.9 \pm 0.1	0.9 \pm 0.2	-0.4 \pm 0.1	0.7 \pm 0.2	-0.8 \pm 0.1	0.9 \pm 0.2
$U_{2m, ZAC}$ $U_{10m, ZAC}$	AWS	-0.9 \pm 0.1	1.5 \pm 0.3	-0.5 \pm 0.1	0.8 \pm 0.2	-0.5 \pm 0.0	0.6 \pm 0.1	-0.7 \pm 0.1	0.8 \pm 0.2
	RACMO	-1.1 \pm 0.1	1.4 \pm 0.3	-0.5 \pm 0.1	0.5 \pm 0.2	-0.3 \pm 0.0	0.4 \pm 0.1	-0.5 \pm 0.1	0.6 \pm 0.2
$q_{2m, ZAC}$	AWS	-0.3 \pm 0.0	0.4 \pm 0.1	-0.5 \pm 0.1	0.5 \pm 0.1	0.1 \pm 0.1	-0.1 \pm 0.1	-0.8 \pm 0.1	0.5 \pm 0.1
	RACMO	-0.1 \pm 0.0	0.2 \pm 0.1	-0.4 \pm 0.1	0.4 \pm 0.1	0.3 \pm 0.1	-0.2 \pm 0.1	-0.6 \pm 0.1	0.4 \pm 0.1
CCF _{M3}	AWS	-22.6 \pm 2.2	23.7 \pm 2.8	-22.6 \pm 2.1	23.6 \pm 2.8	-23.1 \pm 1.8	25.5 \pm 2.9	-20.5 \pm 2.4	20.3 \pm 2.5
	RACMO	-17.0 \pm 3.1	20.5 \pm 2.5	-22.1 \pm 3.2	20.0 \pm 2.5	-14.6 \pm 2.8	17.4 \pm 2.8	-18.9 \pm 3.0	16.2 \pm 2.4
CCF _{ZAC}	AWS	-4.2 \pm 3.1	13.8 \pm 4.4	-5.0 \pm 2.1	11.6 \pm 4.0	-4.7 \pm 3.2	8.7 \pm 3.6	-9.9 \pm 2.8	11.5 \pm 2.8
	RACMO	-10.0 \pm 4.8	21.0 \pm 5.9	-17.3 \pm 4.2	20.6 \pm 4.3	-13.8 \pm 4.0	15.3 \pm 4.0	-19.2 \pm 4.3	16.2 \pm 3.3
$T_{2m, M3}$	AWS	0.4 \pm 0.6	0.7 \pm 0.6	-1.2 \pm 0.7	1.4 \pm 0.6	2.5 \pm 0.4	-2.8 \pm 0.3	-3.2 \pm 0.6	1.8 \pm 0.4
	RACMO	0.8 \pm 0.6	0.5 \pm 0.6	-1.8 \pm 0.7	1.9 \pm 0.5	1.3 \pm 0.4	-1.8 \pm 0.3	-2.8 \pm 0.6	1.8 \pm 0.5
$T_{2m, ZAC}$	AWS	-4.0 \pm 0.5	4.7 \pm 0.6	-5.6 \pm 0.7	4.7 \pm 0.6	-0.8 \pm 0.3	-0.3 \pm 0.3	-7.2 \pm 0.6	4.4 \pm 0.4
	RACMO	0.6 \pm 0.5	0.7 \pm 0.6	-2.0 \pm 0.7	2.0 \pm 0.5	0.8 \pm 0.4	-1.4 \pm 0.3	-3.1 \pm 0.6	2.0 \pm 0.5

Table S5. Mean anomalies of slope temperature gradient (STG in $^{\circ}\text{C km}^{-1}$) and temperature difference (ΔT in $^{\circ}\text{C}$) computed from AWSs pair corresponding to high and low fractional sea-ice cover (SIF in %) from ERA5 averaged over the Greenland Sea for the given season. Temperature gradients and SIF anomalies are calculated using the same period i.e., when the variable is recorded by both AWSs.

Station pairs	Seasons	DJF		MAM		JJA		SON	
	Composites	High	Low	High	Low	High	Low	High	Low
M6-ZAC	Total days	361		368		396		447	
	SIF (days)	34 (18)	-33 (17)	24 (19)	-32 (19)	29 (20)	-6 (270)	32 (23)	-6 (259)
	STG _{M6-ZAC}	2.7	-1.2	1.5	-1.7	2.4	-0.6	-0.5	-1.2
AP1-ZAC	Total days	802		1073		1096		1071	
	SIF (days)	44 (41)	-22 (41)	37 (54)	-35 (54)	32 (55)	-5 (746)	34 (53)	-3 (789)
	STG _{AP1-ZAC}	3.0	-2.9	1.9	-2.1	3.6	-1.0	5.0	-1.8
DAN-ZAC	Total days	1209		1159		1115		1380	
	SIF (days)	49 (59)	-36 (60)	41 (58)	-43 (57)	39 (56)	-9 (581)	45 (69)	-6 (902)
	$\Delta T_{\text{DAN-ZAC}}$	0.9	-0.5	1.3	-0.6	0.9	-0.1	0.1	-0.1
AP2-AP1	Total days	708		957		1043		939	
	SIF (days)	44 (36)	-23 (36)	36 (45)	-36 (47)	32 (53)	-5 (696)	36 (47)	-3 (711)
	STG _{AP2-AP1}	1.4	-2.2	1.9	-2.4	3.0	-0.6	2.5	-0.6
AP3-AP1	Total days	503		703		761		755	
	SIF (days)	39 (26)	-15 (26)	40 (35)	-31 (36)	26 (38)	-4 (530)	30 (38)	-2 (603)
	STG _{AP3-AP1}	-0.2	-1.6	1.5	-1.3	0.4	-0.1	0.4	-0.2

Table S6. Mean anomalies of near-surface variables like wind speed (U_{2m} in m s^{-1}), and specific humidity (q_{2m} in g kg^{-1}) measured and derived from AWS corresponding to high and low fractional sea-ice cover (SIF in %) from ERA5 averaged over the Greenland Sea for the given season. The climate variables and SIF anomalies are calculated using the same period i.e., when the variable is recorded by both AWSs. The AWS which do not record the given variable is not shown.

SIF (%) and U_{2m} (m s^{-1}) anomalies								
Seasons (days)	DJF (1098)		MAM (1115)		JJA (1333)		SON (1406)	
Composites	High	Low	High	Low	High	Low	High	Low
SIF (days)	41 (55)	-25 (73)	35 (56)	-37 (56)	33 (67)	-6 (837)	33 (71)	-5 (965)
$U_{2m, M3}$	-0.3	1.4	-0.9	0.4	-0.4	0.1	0.2	0.1
$U_{2m, ZAC}$	-0.2	0.5	-0.4	0.5	-0.6	0.2	-0.2	0.08

SIF (%) and q_{2m} (g kg^{-1}) anomalies								
Seasons (days)	DJF (2163)		MAM (2206)		JJA (2188)		SON (2184)	
Composites	High	Low	High	Low	High	Low	High	Low
SIF (days)	51 (109)	-35 (111)	42 (109)	-42(111)	38 (110)	-9 (1187)	43 (110)	-6 (1424)
$q_{2m, ZAC}$	-0.3	0.4	-0.7	0.6	-0.8	0.2	-0.9	0.4

References

- Citterio, M., van As, D., Ahlstrøm, A. P., Andersen, M. L., Andersen, S. B., Box, J. E., Charalampidis, C., Colgan, W. T., Fausto, R. S., Nielsen, S., and Veicherts, M.: Automatic weather stations for basic and applied glaciological research, *GEUS Bull.*, 33, 69–72, <https://doi.org/10.34194/geusb.v33.4512>, 2015.
- iMet-XQ2 Second-Generation Atmospheric Sensor for UAV Deployment:
https://www.intermetsystems.com/ee/pdf/202021_iMet-XQ2_210415.pdf, last access: 10 August 2021.
- Kandrup, N. and Iversen, K. M.: *ClimateBasis Manual for ZERO-Version 1*, 1–37 pp., 2010.
- Skov, K., Sigsgaard, C., Mylius, M. R., and Lund, M.: *GeoBasis Guidelines and sampling procedures for the geographical monitoring programme of Zackenberg Basic* This edition of the GeoBasis Manual, 1–186 pp., 2019.